

EVALUATION OF SENSOR PLACEMENT ALGORITHMS FOR ON-ORBIT IDENTIFICATION OF SPACE PLATFORMS¹

Robin S. Glassburn
Graduate Student
Department of Mechanical Engineering
University of Kentucky
Lexington, Kentucky 40506-0046

Suzanne Weaver Smith
Assistant Professor
Department of Engineering Mechanics
University of Kentucky
Lexington, Kentucky 40506-0046

ABSTRACT

Anticipating the construction of the international space station, on-orbit modal identification of space platforms through optimally placed accelerometers is an area of recent activity. Unwanted vibrations in the platform could affect the results of experiments which are planned. Therefore, it is important that sensors (accelerometers) be strategically placed to identify the amount and extent of these unwanted vibrations, and to validate the mathematical models used to predict the loads and dynamic response. Due to cost, installation, and data management issues, only a limited number of sensors will be available for placement. This work evaluates and compares four representative sensor placement algorithms for modal identification. Most of the sensor placement work to date has employed only numerical simulations for comparison. This work uses experimental data from a fully-instrumented truss structure which was one of a series of structures designed for research in dynamic scale model ground testing of large space structures at NASA Langley Research Center. Results from this comparison show that for this cantilevered structure, the algorithm based on Guyan reduction is rated slightly better than that based on Effective Independence.

INTRODUCTION

Monitoring the vibration characteristics of orbiting space platforms such as the international space station has received considerable recent attention. Proposed designs of space platforms that use flexible truss structures to connect operating modules and moving elements (i.e., science and habitation modules, solar panels and radiators) require that activities and experiments performed on-orbit not be disturbed by vibrations induced by motors, positioning thrusters, or other activities. Therefore, an accurate and complete understanding of the vibration characteristics is desired. With this in mind, the Modal Identification Experiment (MIE) was proposed for Space Station Freedom (SSF) to provide frequencies, mode shapes, and damping estimates for model verification (Ref. 1,2).

Before any platform is launched, extensive finite element models will anticipate the structure's vibration performance. In order to verify these finite element models, on-orbit modal identification must be performed. Such testing can not be accomplished on the ground, however, due to the platform's size and flexibility. To address this difficulty, testing of hybrid-scale models has been proposed for initial validation efforts (Ref. 3). Even with what verification can be accomplished through these means, on-orbit tests will be required for final verification.

Detecting structural failure due to micrometeoroid impact or other failure mechanisms is also a concern. If, for example, a portion of the truss structure that will connect the various parts of the Space Station Freedom were to be damaged,

¹Supported by a NASA / Kentucky Space Grant Consortium Graduate Fellowship

extensive astronaut Extra Vehicular Activity (EVA) would be required to find and repair the damaged section. Without the ability to locate a damaged section a priori, more risk would be incurred by the EVA astronauts to manually search these large structures. One approach which has shown promise for locating and assessing damage in truss structures is to monitor the vibration characteristics of the truss (Ref. 4).

Modal identification of a structure produces knowledge of its vibration characteristics from time history data. This means that the mode shapes, the damping, and the natural frequencies are determined. Sensor placement for modal identification of large space structures is a relatively recent topic of study with early works presented and published in the late 1980's and early 1990's. To date most of the evaluation and comparison of proposed techniques to date has been accomplished with numerical experiments. One objective of this work is to apply experimental data from a fully-instrumented laboratory truss to evaluate and compare a representative set of sensor placement algorithms. The experimental data involves nonideal conditions and measurement errors that can not be fully simulated in finite-element-model-based numerical experiments.

This work presents four representative sensor placement methods and four criteria to evaluate each method. Frequency response functions (frfs) are used to extract natural frequencies and mode shapes from which displacements were used corresponding to the subset of candidate locations selected by each method. The evaluation criteria applied to these experimental results are compared with those applied to numerical data from only using the finite element model. Conclusions about pretest planning are drawn. Note that this paper presents a portion of a study which provided more detail and also evaluated a fifth method (Ref. 5).

BACKGROUND

Ideally, a large number of sensors, often accelerometers, would be placed on the platform so mode shape characteristics as well as frequencies could then be extracted from time history measurements. However, because the cost of accelerometers that will survive the dynamic launch forces and temperature changes in the on-orbit environment is high, it is necessary to minimize the number of sensors required to monitor the structure's modal characteristics. This implies an optimization algorithm in which we determine the least number of accelerometers needed and the best places for mounting on the structure to accurately describe these modal characteristics. By definition, the normal mode shapes of distinct modes of an analytical model are linearly independent. Therefore, one goal in sensor placement is to have the mode shapes extracted from the limited number of sensors also be linearly independent. For space platform application, the algorithm must also address the characteristically large number of modes with closely-spaced frequencies that these structures possess.

Sensor number and placement questions arise in other fields. For example, sensor placement applications for HVAC systems to control the work environment in large office buildings could address the possibility of the sick building syndrome (Ref. 6). Sensor placement problems also occur in monitoring various manufacturing processes at all levels from raw materials to finished product (Ref. 7). Sensor placement in buildings is also important for studying the effects of earthquakes. This information helps in the design of new buildings and in the reinforcement of existing buildings to withstand the dynamic forces that earthquakes produce.

In each of the applications above, sensors are placed for one of basically three different goals, state estimation, optimal control, or modal identification. The third of these objectives, system identification, is the focus of this work, specifically the issue of number and placement of sensors to identify specified modes for space platforms.

All algorithms in this work use a finite element model as a starting point for selecting sensor locations. For pretest analysis and test design, this may be the primary available information. Each algorithm attempts a suboptimal approach for placing sensors, an optimal solution often only obtainable through an exhaustive search of every different possible combination of sensors. However, in most practical cases, an exhaustive search is computationally intractable. The number of possible configurations which must be addressed and evaluated in such a search is

$$\eta = \frac{I!}{T![(I-T)!]} \quad (1)$$

where,

- η = number of possible sensor location configurations,
- I = the total number of possible sensor locations,
- T = the number of sensors to be placed.

In the small problem of 100 possible locations and given ten sensors to place, 1.7×10^{13} possible configurations result.

Therefore in this paper, algorithms which optimize defined cost functions determine the best positions for sensor placement. In what follows, the sensor configurations are then evaluated using selected criteria to determine the acceptability of the results and to compare the merits of various techniques. In ground experiments, sensors are typically mounted triaxially, with three perpendicular sensors mounted as one unit. For the purpose of comparison of algorithms, however, individual sensor placement is used in this study.

Table 1 is a summary of sensor placement literature for modal identification. The methods are listed in chronological order with the authors in the left-hand column. The methods primarily fall into four categories with exceptions listed in the right-hand column. Note that italicized entries indicate where a previously published method was used for comparison with the new method presented in the cited paper. In addition to these works which present new techniques, Larson, et. al. (Ref. 8,9) conducted recent comparative studies for sensor and actuator placement, one using numerical simulations for the same cantilevered truss from which we use experimental data in what follows.

From the methods presented in Table 1, one representative method was chosen from each of the first four columns for this comparison study. These methods are the Guyan Reduction method described by Penny et al. (Ref. 10), the Effective Independence method described by Kammer (Ref. 11), the Driving Point Residue method described by Parker et al. (Ref. 12), and the Kinetic Energy method described by Chung and Moore (Ref. 13). They are each described in detail in the next section. The Effective Independence method has recently become the most widely used method for placing sensors for on-orbit applications and the standard for comparison for new methods for identification of large space structures.

SENSOR PLACEMENT METHODS

Effective Independence (EI)

Effective Independence is an iterative method which ranks candidate sensor locations according to their contribution to the linear independence of the target modal partition. The target modal partition, ϕ , is an $m \times n$ column matrix of eigenvectors for all the modes of interest, where m represents the number of candidate sensor locations matching the degrees of freedom (DOFs) of the finite element model and n is the number of "target" modes of interest. The Effective Independence method is usually preceded by calculating the kinetic energy contribution of each DOF. The original candidate set of sensor locations is then decreased by eliminating sensors which contribute little to the kinetic energy of the target modes.

Using Kammer's notation (Ref. 11) the Fisher Information Matrix (FIM), A , is computed as $\phi^T \phi$. The eigenvalues, λ , and eigenvectors, ψ , are determined for the FIM,

$$A\psi = \lambda \psi \quad (2)$$

Since the columns in ϕ each represent different modes of the structure, they are linearly independent. Therefore, the eigenvalues of A are real and positive. The eigenvectors are orthogonal and represent n directions in an n -dimensional space which Kammer calls the Absolute Identification Space. Then, an $m \times n$ matrix G is formed in which each column is associated with the corresponding eigenvalue of A ,

$$G = [\phi \psi] ** [\phi \psi] \quad (3)$$

where "***" indicates term by term multiplication (also called the Hadamard or Schur product). An $m \times n$ matrix is constructed to indicate the fractional contribution of the i^{th} sensor location to the j^{th} eigenvalue as

Table 1. Summary of algorithms found for sensor placement for identification.

Note: methods used for comparison are presented in italics.

<i>'Year</i>	<i>Author(s)</i> ^{Reference #}	Reduction Methods	Effective Independence	Driving Point Residue	Kinetic Energy	Other Methods
'78	Shah & Udwardia ^{Ref. 14}					Covariance Matrix Norm
'78	Le Pourhiet & Le Letty ^{Ref. 15}					Error Sensitivity
'87	Salama, et. al. ^{Ref. 16}				KE	Simulated Annealing
'90	Parker, et. al. ^{Ref. 12}			DPR	KE	
'91	L.M.S ^{Ref. 17}			Avg. DPR		
'91	Kammer ^{Ref. 11}		EI		<i>KE</i>	
'92	Flanigan & Botos ^{Ref. 18}	Guyan Red.				
'92	Kammer & Triller ^{Ref. 19}		<i>EI</i> , EI Derivative			
'92	Lim ^{Ref. 20}		EI Derivative			
'92	Penny, et. al. ^{Ref. 10}	Guyan Red.		<i>Avg. DPR</i>		
'93	Lim ^{Ref. 21}		EI Derivative			
'93	Chung & Moore ^{Ref. 13}			Weighted DPR	Weighted KE	
'93	Yao, et. al. ^{Ref. 22}		<i>EI</i>			Genetic Alg.
'94	Liu & Tasker ^{Ref. 23}		<i>EI</i>			Perturbation Variance & <i>DV</i>
'94	Tasker & Liu ^{Ref. 24}		<i>EI</i> & 3 EI Derivatives			
'94	Brillhart & Kammer ^{Ref. 25}		<i>EI</i>		2 KE Methods	
'94	Hemez & Farhat ^{Ref. 26}		<i>EI</i> & EI Derivative			<i>NRG</i>
'94	Johnson & Mack ^{Ref. 27}	A-Set Prioritization			KE	
'94	Pape ^{Ref. 28}	<i>Guyan Red.</i>				Chebyshev Interpolation
'94	Larson, et. al. ^{Ref. 8,9}		<i>EI</i>		<i>KE</i> & <i>Avg. KE</i>	<i>Eigenvector Product</i>

$$F_E = G[\lambda]^{-1} \quad (4)$$

where,

F_E = Fractional Eigenvalue Distribution (m x n).

Finally, a column vector (m x 1) of the effective independence values is calculated as follows,

$$E_D = \left[\sum_{j=1}^k F_{E1j} : \sum_{j=1}^k F_{E2j} : \dots : \sum_{j=1}^k F_{Esj} \right]^T \quad (5)$$

where,

E_D = Effective Independence Distribution,

in which the i^{th} term in the column vector is the fractional contribution of the i^{th} sensor to the linear independence of the modal partitions.

Values in the vector E range from 0.0 to 1.0. A value of 0.0 indicates that the candidate sensor location does not provide independent information and is not observable from its location. Conversely, a value of 1.0 indicates that sensor location must be retained in order to identify the target modes in the columns of ϕ . In application, values are between these limits, so a threshold must be established to select those sensors contributing the most to the linear independence. The EI values for all candidate locations are sorted and the location with the lowest value is removed. The process then iterates though these steps beginning with determining the new FIM from the finite element model using only the remaining sensor candidates. At each iteration only one sensor candidate is removed.

Guyan Reduction (GU)

The Guyan Reduction sensor placement method came about as a result of the work of Guyan (Ref. 29), who devised a method in 1965 which is used to reduce the size of finite element models, namely stiffness and mass matrices. This placement method works by eliminating those DOF for which the inertia forces are negligible compared with the elastic forces. This is an iterative process where during each iteration one "slave" DOF is defined as the DOF with the largest ratio of stiffness to inertia and the remaining DOFs are termed "master" DOFs. The stiffness and mass matrices for the structure's matrix eigenproblem are reordered and partitioned,

$$\left\{ \begin{bmatrix} S_{mm} & S_{ms} \\ S_{sm} & S_{ss} \end{bmatrix} - \omega^2 \begin{bmatrix} M_{mm} & M_{ms} \\ M_{sm} & M_{ss} \end{bmatrix} \right\} \begin{Bmatrix} \delta_m \\ \delta_s \end{Bmatrix} = \begin{Bmatrix} 0 \\ 0 \end{Bmatrix} \quad (6)$$

where,

$[\delta]$ = reordered and partitioned eigenvector,

$[S]$ = stiffness matrix,

$[M]$ = mass matrix,

mm = matrix partition corresponding to master DOFs (m x m),

ss = matrix partition corresponding to slave DOF (s x s),

ms,sm = vectors m x s and s x m, respectively,

s = number of slave DOFs = 1,

ω^2 = eigenvalue.

Henshell and Ong (Ref. 30) present the constraint equation from the slave partition,

$$\{\delta_s\} = -[S_{ss}]^{-1}[S_{sm}]\{\delta_m\} \quad (7)$$

which is used in the strain and kinetic energy equations for the structure to produce the reduced stiffness and mass

$$[S^*] = [S_{mm}] - [S_{ms}][S_{ss}]^{-1}[S_{sm}] \quad (8)$$

$$[M^*] = [M_{mm}] - [S_{ms}][S_{ss}]^{-1}[M_{sm}] - [M_{ms}][S_{ss}]^{-1}[S_{sm}] + [S_{ms}][S_{ss}]^{-1}[M_{ss}][S_{ss}]^{-1}[S_{sm}] \quad (9)$$

where,

[S*] = the reduced stiffness matrix, and

[M*] = the reduced mass matrix.

The new reduced model is ready for the next iteration and the iterations continue until the number of master DOFs remaining equals the number of allowed sensor locations. Henshell and Ong (Ref. 30) suggest only the diagonals of the stiffness and mass matrices be used to determine which DOFs are slave and master from the assumption that off-diagonal terms in the stiffness/inertia ratio matrix can be neglected.

Penny, Friswell, and Garvey (Ref. 10) investigated three different structures using the Guyan Reduction algorithm and concluded that this method selected an appropriate subset when the structure was grounded or had no rigid body modes. They also noted that for structures with one or more rigid body modes, the method works adequately but not as well as the Driving Point Residue method which they used for comparison purposes. We are generally interested in free/free structures with rigid body modes, so we expect this method to perform less adequately on-orbit than our experimental results indicate.

Driving Point Residue (DPR)

Another method used to place sensors is by calculating the Driving Point Residue of each DOF. From Parker, Rose, and Brown's paper (Ref. 12), Driving Point Residues are equivalent to modal participation factors, and are a measure of the degree of excitation or participation of each mode in the overall response. Driving Point Residues are proportional to the magnitudes of the resonance peaks in a driving point frequency response function. The Driving Point Residue is calculated for a structure from the following:

$$[DPR] = [\phi] * * [\phi][\omega] \quad (10)$$

where,

[DPR] = Driving Point Residue values for the structure,

[\omega] = matrix of eigenvalues of target modes.

Each element of the DPR matrix represents the Driving Point Residue contribution of that DOF in a particular target mode. Therefore the i^{th} row represents the contributions of the i^{th} DOF to each of the target modes. Since some of these elements can be small or even zero (if at a node of the target mode), the row is averaged and multiplied by the smallest element in that row to produce a "weighted" measure of the Driving Point Residue contribution of each DOF. Since a sensor placed at a node of a mode would not yield useful information, this biases the method against small or zero elements in the DPR matrix.

Kinetic Energy (KE)

The Kinetic Energy approach may be considered the most common approach used to place sensors, since a majority of "Engineering Judgement" in placing sensors is based on it. Typically, those experienced in experimental procedures will look for, among other things, areas of the structure where there is large displacement. These areas would be the best positions for the sensors to observe the behavior of the structure with the largest signal to noise ratios.

Generally, the Kinetic Energy method works by calculating the kinetic energy of each DOF for each mode and then using the DOFs with the largest values as positions for sensor placement. The form used herein takes the equation for the $m \times n$ modal kinetic energy (MKE),

$$[MKE] = [\phi] ** [M][\phi] \quad (11)$$

and produces a weighted form once again with the weighted average equal to the average value for the row times the minimum value in that row.

EVALUATION CRITERIA

In order to compare the selected methods, four evaluation criteria are presented. The criteria were designed to judge the ability of a sensor set to accurately determine the mode shapes and natural frequencies of the structure.

Modal Assurance Criteria

The first two criteria involve the Modal Assurance Criterion (MAC). The MAC is used to present a measure of orthogonality between two eigenvectors (or extracted mode shapes), as,

$$MAC_{ij} = \frac{\phi_i^T \phi_j}{\sqrt{\phi_i^T \phi_i} \sqrt{\phi_j^T \phi_j}} \quad (12)$$

where,

$\phi_i, \phi_j = i^{\text{th}}, j^{\text{th}}$ mode shape vector,

MAC values range from 0 to 1 with 0 indicating that the two vectors are independent. Generally the MACs are presented in a matrix for $i, j = 1, \dots, n$. From this matrix, two criteria are derived. First, the maximum off-diagonal MAC value is determined. Second, the root-mean-square (RMS) of the off-diagonal elements is computed.

Determinant of the Fisher Information Matrix

The determinant of the Fisher Information Matrix (FIM) was selected as a criteria because it is used as an objective function in one method (Ref. 22) and is the inverse of the Covariance Matrix of the estimate error. The estimate error is the difference between the real target mode response and the estimated response (Ref. 11,22). The goal is to minimize the estimate error by maximizing the determinant of the FIM. The FIM is given by,

$$Q = \frac{1}{\chi^2} \phi^T \phi \quad (13)$$

Where,

$\chi^2 =$ variance of stationary Gaussian white noise.

The same effect is achieved by maximizing the determinant of the numerator of the MAC described above,

$$A = \phi^T \phi \quad (14)$$

SVD Ratio

A singular value decomposition of the eigenvector matrix, ϕ , is determined and the ratio of the largest to smallest value is computed. The SVD ratio takes into account three quantities: mode orthogonality, the condition of the mode expansion problem, and the observability of the modes (Ref. 10). If a singular value is close to zero, the indication is that one mode shape is not independent of the others. With increasing independence, the SVD ratio of highest to lowest is lowered.

NASA 8-BAY TRUSS EXPERIMENTS

Experimental data from an 8-bay cantilevered laboratory truss was intended to provide a large database for use in validation of proposed methods for on-orbit model verification and damage detection in flexible truss structures (Ref. 31). The truss was part of the hybrid-scaled structure designed for the Dynamic Scale Model Technology research program at NASA Langley Research Center (Ref. 3) and exhibits desired response characteristics of closely-spaced frequencies and light damping. Each bay is 0.5 m (19.685 in.) on a side. The truss was mounted to a rigid backstop plate.

The finite element model for this structure consisted of 32 nodes and 96 DOFs as illustrated in Figure 1. The truss was modeled with rod elements that carry only axial load and concentrated masses for the nodes and instrumentation. Node numbering starts at the free end.

Acceleration time history data was collected at each node in each of the three orthogonal reference-axes directions using accelerometers and two driving points which were excited with a burst random pattern as detailed in NASA TM-107626 (Ref. 31). In the peaks of the sample frequency response function (frf) shown in Figure 2, representing the response at node 30 (near the fixed end) in the -Z direction to the excitation at node 4 (at the free end) in the +X direction, the first five mode frequencies of the structure are seen. The first five mode shapes, extracted using the polyreference method and all 96 sensors, and are depicted in Figure 3 with the fixed end of the truss at the top in each case. Table 2 compares the first five natural frequencies from the analytical model and experimental results.

Table 2. Frequency values for the analytical model and experimental data.

Mode #	Analytical Freq.(Hz)	Experimental Freq.(Hz)	Description
1	13.925	13.876	1 st X-Y Bending
2	14.441	14.480	1 st Y-Z Bending
3	46.745	48.411	1 st Torsional
4	66.007	64.035	2 nd X-Y Bending
5	71.142	67.465	2 nd Y-Z Bending

Figure 4 shows a representation of the FEA analytical and experimental mode shapes for mode 1. Observe that in the analytical model the X and Z DOFs are equal in magnitude, while in the experimental results the X and Z DOFs are unequal. This is because the principle bending axes between the two models are not aligned. Also note that the data from sensors at DOFs 45 and 84 are suspect. Here 45 can be seen. Small values are predicted by the analytical model in the Y direction and these values therefore show the largest percent differences between analytical and experimental results.

The mode shapes and natural frequencies were first extracted using the full set of frf data. Subsets of these mode displacements were used to evaluate each sensor placement method. In response to the question of how the mode extraction might vary with the sensor set selected, only the frfs corresponding to a chosen sensor set were also used to extract mode shapes and natural frequencies. In general, the percent differences between the modes extracted from the full frf set and those from the selected frf set were less than 1 percent for the X and Z DOFs. Because values in the axial direction of the truss (Y) are small, larger differences (typically under 6 percent though) were noted between the mode shapes extracted from the full set of frfs and the mode shapes extracted from the reduced set. DOF 23 showed a percent difference, however, exceeding 200 percent, due to a sign difference between the extractions. The natural frequencies extracted using each method were identical to two decimal places.

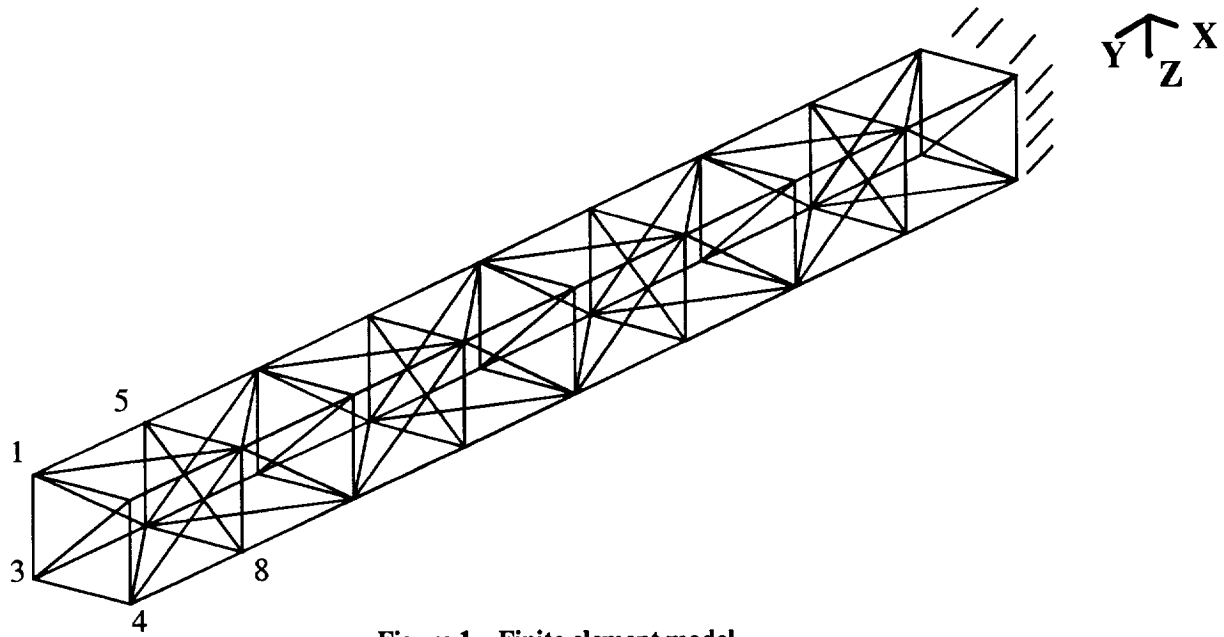


Figure 1. Finite element model

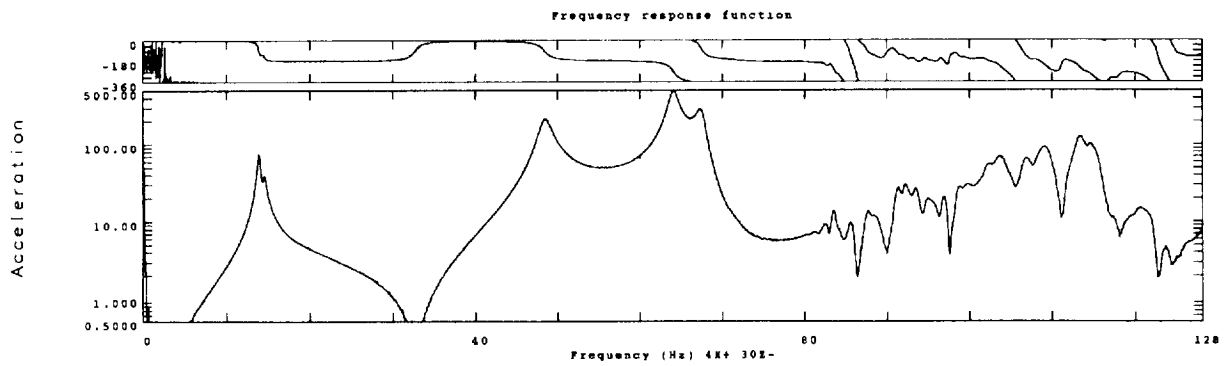


Figure 2. Sample frequency response function

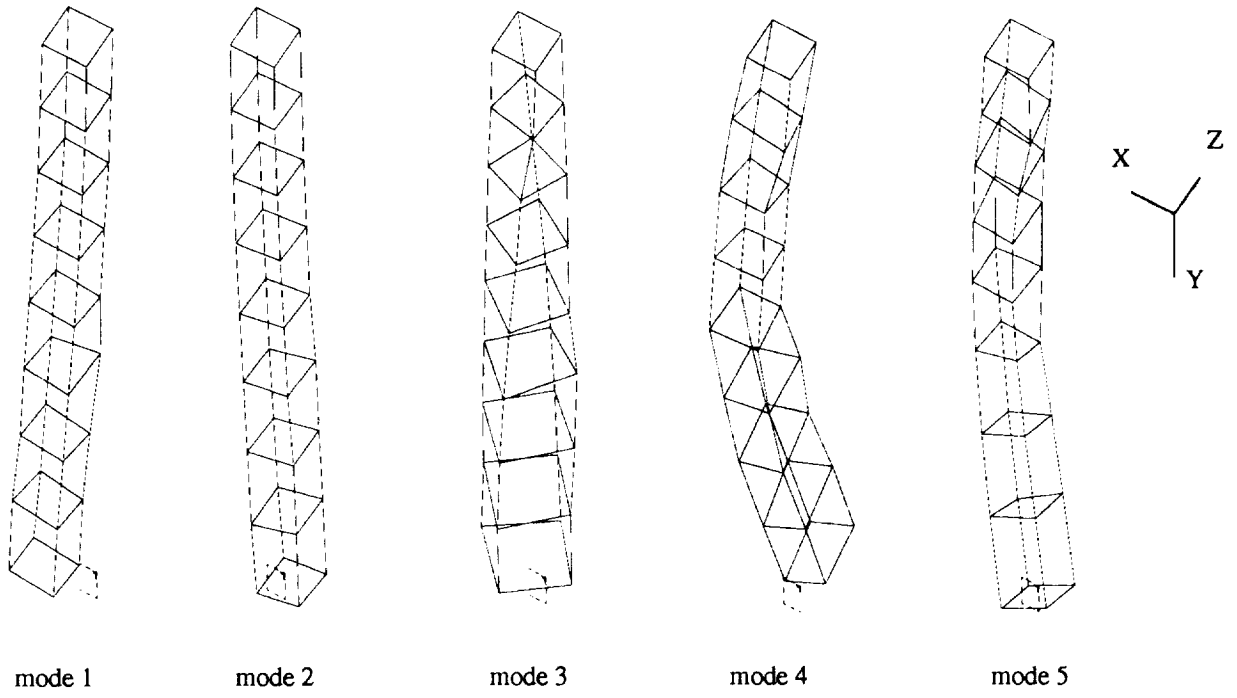


Figure 3. First five mode shapes extracted from test data

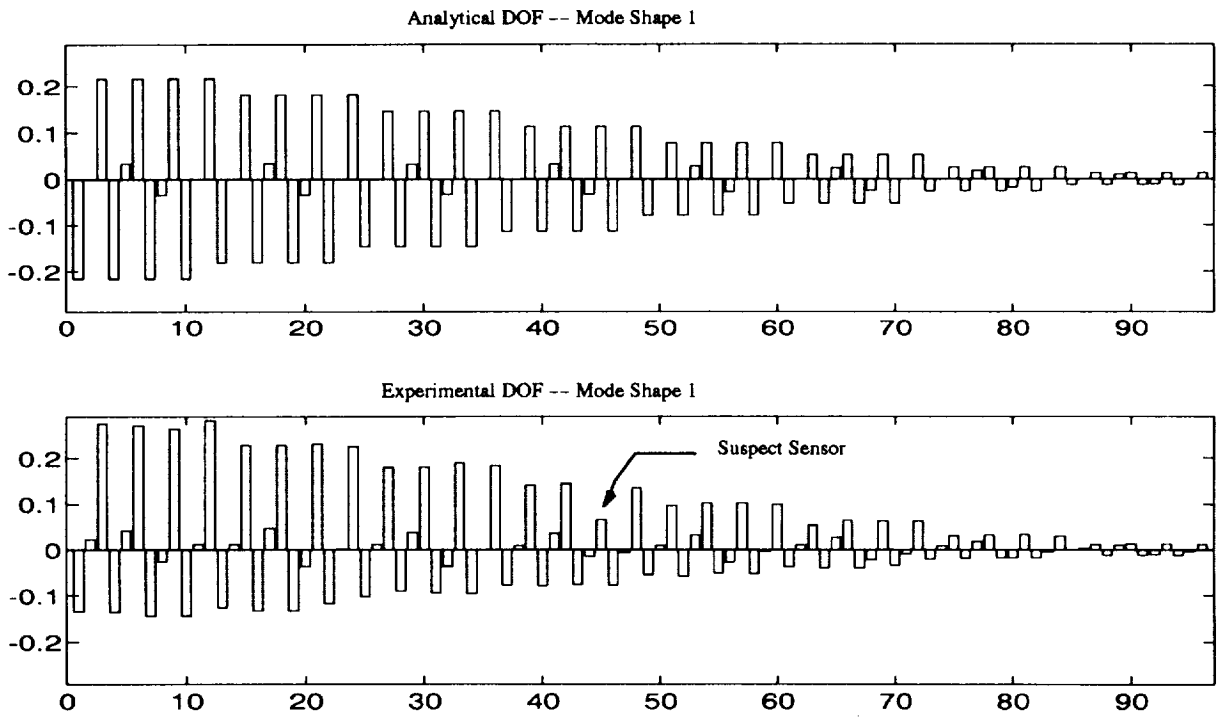


Figure 4. Analytical vs. Experimental mode shape 1

SENSOR PLACEMENT EVALUATIONS

Each of the four methods presented previously were used to select a subset of sensor locations from the full 96-DOF finite element model. Subsets included 5% (5 sensor locations), 10% (10 sensor locations), and 15% (14 sensor locations) of the available DOFs. Ten percent has been suggested as a reasonable number for on-orbit instrumentation (Ref. 32). The 5% and 15% subsets were presented to show the trends of each method. "One sensor minus 10%" (9 sensor locations) and a "one sensor plus 10%" (11 sensor locations) subsets were also evaluated but are not presented here due to the generally small change in evaluation values. It is important to note, however, that between the 10% and the "one plus 10%" subsets for this truss, the SVD ratio and FIM determinant results improved greatly. Figures 5-7 illustrate the sensor locations picked by each method for each case grouped by number of sensor locations. For presentation clarity the diagonal members of the truss are not shown in these figures.

Note that those sensors appearing in the 5% subset are in the 10% subset also and similarly in the 15% subset. So, as iterations or reductions proceed for these four methods, the next iteration or reduction always yields a subset of the previous candidate sensor location set.

In Figures 5-7 placement patterns can be seen for each method. The patterns of sensor locations chosen by the EI and the KE methods are similar. They tend to locate sensors at the mid-section and free-end of the truss, which tends to maximize the observability of the first five modes. In other words, from the mode shapes presented in Figure 2 the maximum displacements are located in these areas. The EI method places more importance on the mid-section of the truss than the KE method as can be seen by comparing Figures 5 and 6.

The GU method distributes the sensor locations over the structure more than the first two methods. Note, however that it also locates sensors at the mid-section and free-end, just not as closely spaced as those from the first two methods. The GU method is also the only method to pick a subset sensor location in the axial (Y) direction from the four methods presented. With the differences between the axial displacements from the analytical model and those from the experimental results, no adverse effect was noticed in the GU subset evaluation results.

The DPR method places sensors at the free-end only. This makes the first mode pair indistinguishable from the second mode pair. As a result, this method performs poorly.

To evaluate each selected sensor subset's performance, the criteria presented above were applied. High values for the FIM determinant and low values for the MAC criteria and the SVD ratio produce a better sensor set. An evaluation was first performed using all of the DOFs to provide a relative measure of the effect of experimental imperfections for the fully instrumented case. These evaluation results are presented in Table 3. Note that the analytical results are slightly better than the experimental results due to modeling error and measurement imperfections. Table 3 is presented to demonstrate experimental effects in the criteria and to give a standard for results which follow.

Table 3 Experimental and Analytical evaluation results using all finite element DOFs.

Evaluation Criteria	Experimental Evaluation Results	Analytical Evaluation Results	Percent Difference
Max MAC	6.455×10^{-3}	4.982×10^{-3}	30%
RMS MAC	2.769×10^{-3}	2.157×10^{-3}	28%
SVD Ratio	1.120	1.073	4%
FIM Determinant	0.985	0.990	5%

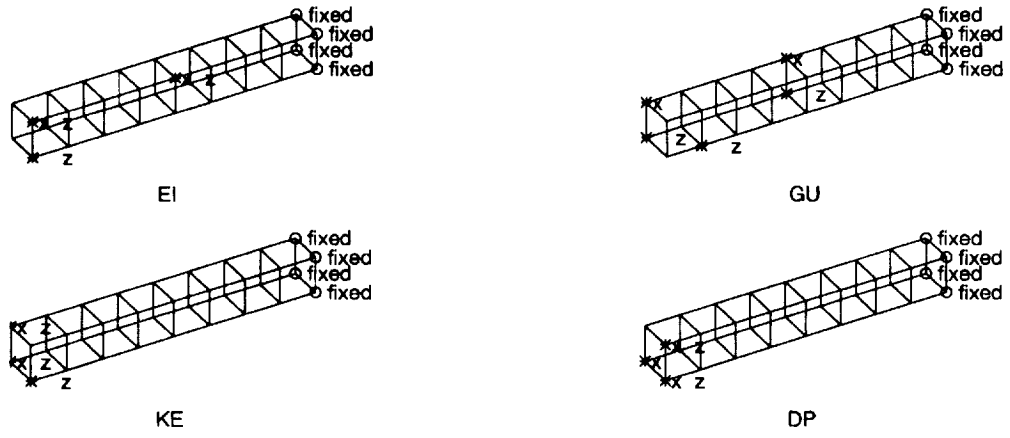


Figure 5. Truss with 5% instrumentation

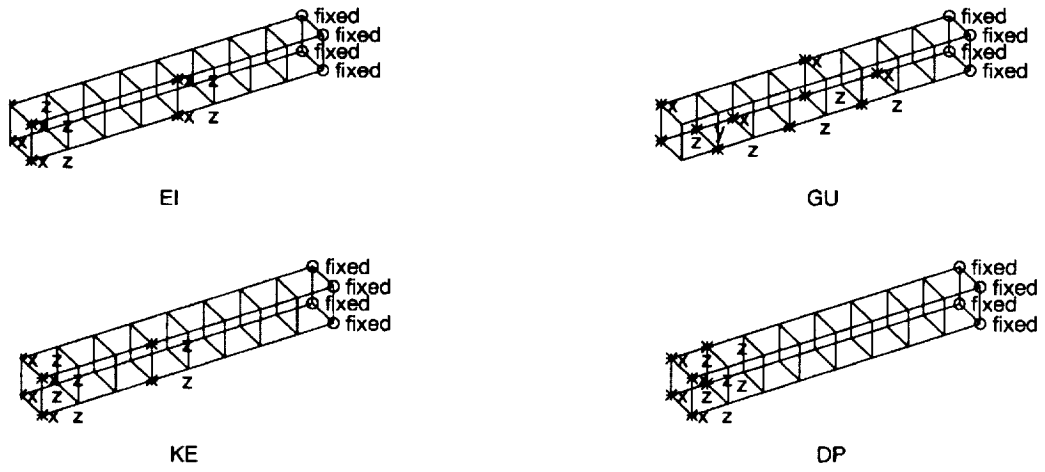


Figure 6. Truss with 10% instrumentation

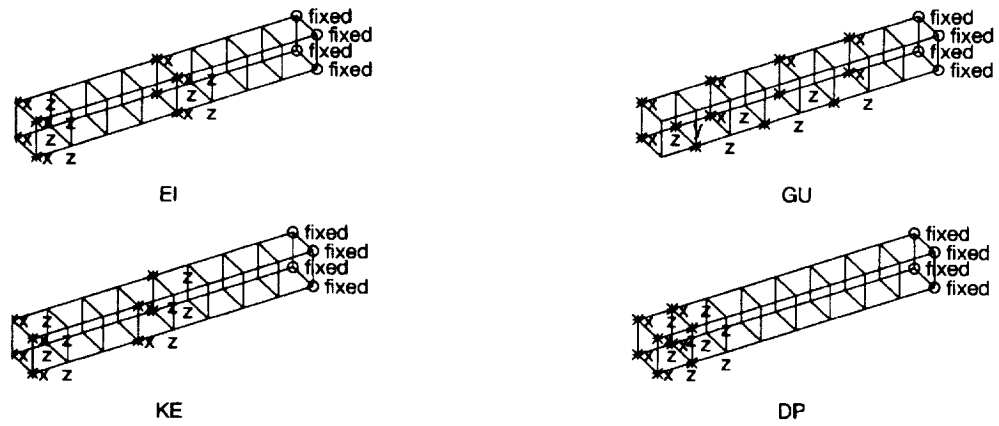


Figure 7. Truss with 15% instrumentation

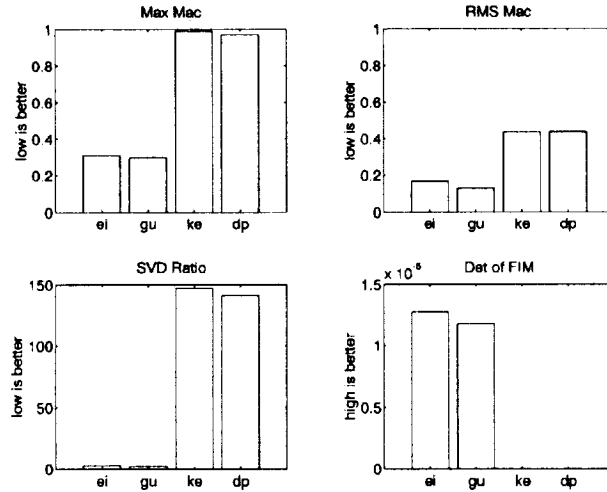


Figure 8. Evaluation results for 5% instrumentation

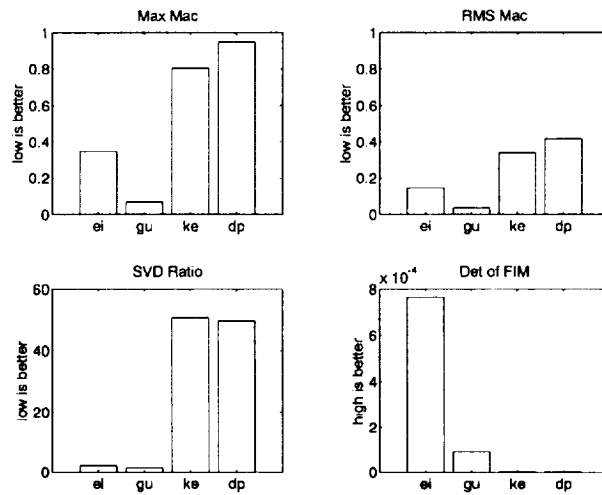


Figure 9. Evaluation results for 10% instrumentation

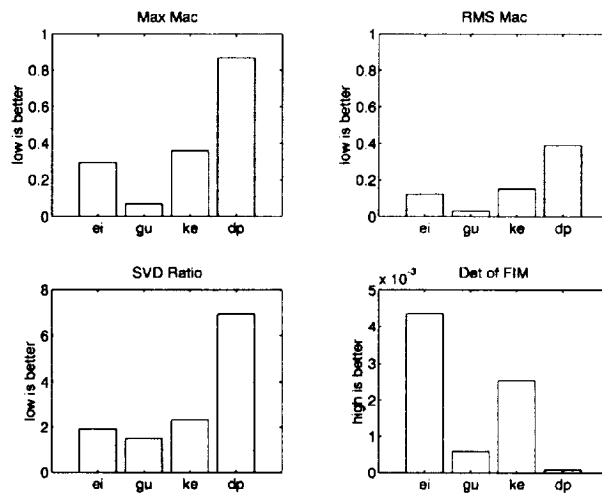


Figure 10. Evaluation results for 15% instrumentation

The evaluation results for the 5%, 10%, and 15% instrumentation cases are presented in Figures 8-10, respectively. The MAC evaluation criteria show the GU subset to have the most efficient sensor placement followed by the EI subset. The KE and the DPR subsets ranked much lower than the first two. It was found in Reference 5 that for grounded structures the GU method picks a subset which is generally better than the others and for free structures the DPR method tends to perform better. Penny et. al. found similar results with the GU method (Ref. 10). Larson (Ref. 9) found that the EI method performed better than the KE methods studied.

The SVD ratio changes dramatically between each of the presented subsets. This is partially due to the discrete nature of optimization which is employed by each of these methods. Adding or subtracting one or more sensors a large change in the identifiability could result. The SVD criteria also selects the GU subset as the best set followed by the EI method.

The FIM determinant, however, shows the EI method performing better for all subsets. The GU method is shown as the next best for the 5% and the 10% instrumentation. The KE subset becomes the second best method in this criteria for sensor sets above 10% (beginning at the "10% plus one" subset). A similar result was found in Reference 5 and it was noted that generally the best methods picked by the MAC criteria and SVD ratio were also picked as top methods by the FIM determinant criteria, but not always in the same order).

These four criteria were also applied to evaluate sensor placements using a numerical free/free and fixed/free square plate (no experimental data available). Results were similar and, as expected, the DPR method was superior to the GU method in the free/free case (Ref. 5).

SUMMARY

Four representative sensor placement methods for modal identification were evaluated using four evaluation criteria. An 8-bay cantilevered laboratory truss was employed to test each method with the evaluation criteria.

The four methods presented were representative of nineteen found in the literature. From these, the GU method produced the most favorable results. The EI method performed second best for this structure. It should be noted, that for free structures the DPR method does generally better than GU as was found in References 5 and 10. Also the EI method performed better than the KE method as was found in Reference 9. The KE and DPR produced evaluation results that were similar for 5% and 10% instrumentation. Above 10% instrumentation, the KE method performs better than both the GU and DPR methods considering the FIM determinant criteria.

All methods were designed for modal identification and evaluated for this purpose as well. However, for damage detection, different placement approaches and evaluation criteria may be needed. In particular, more axial measurements may be required. The axial sensor locations for this truss structure were found to produce relatively large differences between the analytical and experimental results. More sensitive instrumentation should be used for these measurements if required for damage detection.

REFERENCES

1. Kim, H.M. and Doiron, H.H., "On-Orbit Modal Identification of Large Space Structures," *Sound and Vibration*, Vol. 26, No. 6, June 1992, pp. 24-30.
2. Kim, H.M. and Doiron, H.H., "Modal Identification Experiment Design for Large Space Structures," *AIAA/ASME/ASCE/AHS/ASC 32nd Structures, Structural Dynamics, and Materials Conference*, Baltimore, MD., April 1991, pp. 2968-2976.
3. McGowan, P.E., Javeed, M., and Edighoffer, H.H., "Status of Dynamic Scale Model Technology Research Program," *NASA Technical Memorandum 102764*, Jan. 1991.

4. Smith, S.W. and Hendricks, S.L., "Damage Detection and Location in Large Space Trusses," *AIAA SDM Issues of the International Space Station, A Collection of Technical Papers*, Williamsburg, Va., April 21-22, 1988, pp. 56-63.
5. Glassburn, R.S., "Evaluation of Sensor Placement Algorithms for On-Orbit Identification of Space Platforms," Masters Thesis - University of Kentucky, Lexington, Kentucky 1994.
6. Triplett, T., "Is There Trouble in The Air?," *Safety and Health*, Vol. 145, No. 5, May 1992, pp. 38-44.
7. "MRP II Software Provides Flexibility for Manufacturer," *Industrial Engineering*, Vol. 24, No. 11, Nov. 1992, pp. 25.
8. Larson, C.B., Zimmerman, D.C., and Marek, E.L., "A Comparative Study of Pre-Test Techniques using the NASA 8-bay Truss," *Proceedings of the 12th International Modal Analysis Conference*, Honolulu, Hawaii, Jan.-Feb. 1994, pp. 205-211.
9. Larson, C.B., Zimmerman, D.C., and Marek, E.L., "A Comparative Study of Metrics for Modal Pre-Test Sensor and Actuator Selection Using the JPL/MPI Testbed Truss," *Proceedings of the AIAA Dynamics Specialists Conference*, Hilton Head, S.C., April 21-22 1994, pp. 150-162.
10. Penny, J.E.T., Friswell, M.I., and Garvey, S.D., "The Automatic Choice of Measurement Locations for Dynamic Testing," *Proceedings of the 10th International Modal Analysis Conference*, San Diego, Ca., Feb. 1992, pp. 30-36.
11. Kammer, D.C., "Sensor Placement for On-Orbit Modal Identification and Correlation of Large Space Structures," *Journal of Guidance, Control, and Dynamics*, Vol. 14, No. 2, March-April 1991, pp. 251-259.
12. Parker, G.R., Rose, T.L., and Brown, J.J., "Kinetic Energy Calculation as an Aid to Instrumentation Location in Modal Testing," *Proceedings of the 1990 MacNeal-Schwendler Corporation World Users Conference*, Los Angeles, Ca., March 28-30, 1990.
13. Chung, Y. and Moore, J.D., "On-Orbit Sensor Placement and System Identification of Space Station with Limited Instrumentation," *Proceedings of the 11th International Modal Analysis Conference*, Kissimmee, Florida, Feb. 1993, pp. 41-46.
14. Shah, P.C. and Udawadia, F.E., "A Methodology for Optimal Sensor Locations for Identification of Dynamic Systems," *Journal of Applied Mechanics*, Vol. 45, No. 3, March 1978, pp. 188-196.
15. Le Pourhiet, A. and Le Letty, L., "Optimization of Sensor Locations in Distributed Parameter System Identification," Identification and System Parameter Estimation, Rajbman (ed.), North-Holland Co., 1978, pp. 1581-1592.
16. Salama, M., Rose, T., and Garba, J., "Optimal Placement of Excitations and Sensors for Verification of Large Dynamical Systems," *Proceedings of the AIAA/ASME/ASCE/AHS 28th Structures, Structural Dynamics and Materials Conference*, Monterey, Ca., April 1987, pp. 1024-1031.
17. LMS International, "Large-Scale Modal Testing of a Space Frame Structure - from Pretest Analysis to FEA Model Validation," *Sound and Vibration*, Vol. 25, No. 3, March 1991, pp. 6-16.
18. Flanigan, C.C. and Botos, C.D., "Automated Selection of Accelerometer Locations for Modal Survey Tests," *Proceedings of 10th International Modal Analysis Conference*, San Diego, California, Feb. 1992, pp. 1205-1208.

19. Kammer, D.C. and Triller, M.J., "Efficient Sensor Placement for On-Orbit Modal Identification of Sequentially Assembled Large Space Structures," *Proceedings of the 10th International Modal Analysis Conference*, San Diego, Ca., Feb. 1992, pp. 954-964.
20. Lim, T.W., "Sensor Placement for On-Orbit Modal Testing," *Journal of Spacecraft and Rockets*, Vol. 29, No. 2, March-April 1992, pp. 239-246.
21. Lim, T.W., "Actuator/Sensor Placement for Modal Parameter Identification of Flexible Structures," *International Journal of Analytical and Experimental Modal Analysis*, Vol. 8, No. 1, Jan. 1993, pp. 1-13.
22. Yao, L., Sethares, W.A., and Kammer, D.C., "Sensor Placement for On-Orbit Modal Identification via a Genetic Algorithm," *AIAA Journal*, Vol. 31, No. 10, Oct. 1993, pp. 1922-1928.
23. Liu, C. and Tasker, F.A., "Sensor Placement Using Time Domain Perturbation Approach," *Proceedings of the AIAA Dynamics Specialists Conference*, Hilton Head, S.C., April 21-22 1994, pp. 163-172.
24. Tasker, F.A. and Liu, C., "Extended Variance-Based Techniques for Sensor Placement in Modal Identification," *Proceedings of the AIAA Dynamics Specialists Conference*, Hilton Head, S.C., April 21-22 1994, pp. 173-181.
25. Brillhart, R.D. and Kammer, D.C., "Evaluation of Optimal Modal Sensor Placement Using a System Realization Method," *Proceedings of the 12th International Modal Analysis Conference*, Honolulu, Hawaii, Jan.-Feb. 1994, pp. 1401-1407.
26. Hemez, F.M. and Farhat, C., "An Energy Based Optimum Sensor Placement Criterion and Its Application to Structural Damage Detection," *Proceedings of the 12th International Modal Analysis Conference*, Honolulu, Hawaii, Jan.-Feb. 1994, pp. 1568-1575.
27. Johnson, C.L. and Mack, N., "Accelerometer Selection for the Modal Survey of the Space Station Combined Cargo Element," *Proceedings of the 12th International Modal Assurance Conference*, Honolulu, Hawaii, Jan.-Feb. 1994, pp. 1230-1236.
28. Pape, D.A., "Selection of Measurement Locations for Experimental Modal Analysis," *Proceedings of the 12th International Modal Analysis Conference*, Honolulu, Hawaii, Jan.-Feb. 1994, pp. 34-41.
29. Guyan, R.J., "Reduction of Stiffness and Mass Matrices," *AIAA Journal*, Vol. 3, No. 2, Feb. 1965, pp. 380.
30. Henshell, R.D. and Ong, J.H., "Automatic Masters for Eigenvalue Economization," *International Journal of Earthquake Structural Dynamics*, Vol. 3, 1975, pp. 375-383.
31. Kashangaki, T., "Ground Vibration Tests of a High Fidelity Truss for Verification of On-Orbit Damage Location Techniques," *NASA Technical Memorandum 107626*, May 1992.
32. Pappa, R.S., "Some Instrumentation Requirement Issues for the Space Station Structural Characterization Experiment," *Presented at the USAF/NASA Workshop on Model Determination for Large Space Systems*, Pasadena, Ca., March 22-24 1988.